

# Prediction of anomalies in the velocity of sound for the pseudogap of hole-doped cuprates

C. Walsh,<sup>1</sup> M. Charlebois,<sup>2</sup> P. Sémon,<sup>3</sup> G. Sordi,<sup>1,\*</sup> and A.-M. S. Tremblay<sup>3</sup>

<sup>1</sup>*Department of Physics, Royal Holloway, University of London, Egham, Surrey, UK, TW20 0EX*

<sup>2</sup>*Département de Chimie, Biochimie et Physique, Institut de Recherche sur l'Hydrogène, Université du Québec à Trois-Rivières, Trois-Rivières, Québec, Canada G9A 5H7*

<sup>3</sup>*Département de physique, Institut quantique & RQMP, Université de Sherbrooke, Sherbrooke, Québec, Canada J1K 2R1*

(Dated: July 5, 2022)

We predict sound anomalies at the doping  $\delta^*$  where the pseudogap ends in the normal state of hole-doped cuprates. Our prediction is based on the two-dimensional compressible Hubbard model using cluster dynamical mean-field theory. We find sharp anomalies (dips) in the velocity of sound as a function of doping and interaction. These dips are a signature of supercritical phenomena, stemming from an electronic transition without symmetry breaking below the superconducting dome. If experimentally verified, these signatures may help to solve the fundamental question of the nature of the pseudogap – pinpointing its origin as due to Mott physics and resulting short-range correlations.

*Introduction.*– Upon decreasing the temperature near half-filling, cuprate superconductors reach a temperature  $T^*$  where most transport, thermodynamic, and photoemission experiments show features that suggest a loss in the density of states. This has been associated to a so-called pseudogap phase, with  $T^*$  a crossover rather than a sharp phase transition<sup>1</sup>. On the other hand, in 2018, experiments revealed that thermodynamic properties show signatures of a phase transition upon crossing the critical doping  $\delta^*$  where the pseudogap ends at low temperature, such as a sharp peak in the specific heat<sup>2</sup>. Even more puzzling, this thermodynamic signature of a transition occurs without a detectable diverging correlation length associated to a broken symmetry state<sup>1,2</sup>. Detected broken symmetries are not consistent with gap opening or a drop in carrier densities<sup>1</sup>. Furthermore, broken symmetry states, such as superconductivity and charge density waves, may develop within the pseudogap phase<sup>1,3</sup>.

The two-dimensional (2D) Hubbard model in the doped Mott insulator regime<sup>4</sup> captures these aforementioned key features that are consistent with the observed pseudogap – namely (i) that the pseudogap is a crossover across  $T^*$  and (ii) there is a phase transition across  $\delta^*$  at low  $T$ , (iii) without the need of a broken symmetry state, (iv) which can however appear within the pseudogap phase. In particular, studies on this model based on cluster extensions of dynamical mean-field theory<sup>5</sup> revealed that the phase transition across  $\delta^*$  is a metal to metal first-order transition without symmetry breaking<sup>6,7</sup>, due to Mott physics and short range correlations. This transition ends at finite doping and finite temperature in a second order critical point, from which supercritical crossovers emerge<sup>8,9</sup>. This theoretical framework resolves the paradox of the thermodynamic anomalies at the endpoint of the pseudogap (e.g. the peak in the specific heat across  $\delta^*$ ) without the need for broken symmetry states, as discussed in Refs.<sup>10,11</sup>.

In this article we provide a novel and crucial *prediction* of this theoretical framework for ultrasound experiments

in hole-doped cuprates. The propagation of sound is a powerful tool to characterise phase transitions in solids because it is a sensitive way of probing the thermodynamics of a system. We shall prove that the velocity of sound has signatures of a phase transition across  $\delta^*$  and of a crossover across  $T^*$ . Crucially, if confirmed by experiments, this will provide further decisive evidence that the pseudogap arises from Mott physics and short-range correlations.

Recent advances in ultrasound techniques should enable the testing of our prediction. Indeed, the last few years have witnessed a renewed attention in using ultrasounds to probe electronic phase transitions in strongly correlated electron systems, and experimental findings motivate new theoretical investigations. For example, an experiment<sup>12</sup> in the cuprate  $\text{YBa}_2\text{Cu}_3\text{O}_{6+x}$  (YBCO) found a break in the slope of the velocity of sound at the onset of the pseudogap, suggestive of a phase transition, although this interpretation has been challenged in Ref.<sup>13</sup>. In another cuprate,  $\text{La}_{2-x}\text{Sr}_x\text{CuO}_4$  (LSCO), ultrasound anomalies were connected to the coupling between the lattice and the spin glass<sup>14,15</sup>. In other correlated electron systems, ultrasounds were used to place constraints on the order parameter symmetry of the hidden order in  $\text{URu}_2\text{Si}_2$ <sup>16</sup> and in the superconducting state of  $\text{Sr}_2\text{RuO}_4$ <sup>17,18</sup>. Anomalies in the velocity of sound have been used to describe the crossover emerging from the Mott transition in  $\text{V}_2\text{O}_3$ <sup>19</sup> and organic superconductors<sup>20,21</sup>. Our contribution in this article is to identify how the velocity of sound captures the pseudogap emerging from Mott physics and resulting short-range correlations.

*Model and method.*– The velocity of sound  $c_s$  along high symmetry directions is defined as  $c_s = \sqrt{c_{ij}/\rho}$ , where  $\rho$  is the density,  $c_{ij} = \partial^2 F / \partial u_{ij}^2$  is the elastic constant in the Voigt notation,  $F$  is the free energy, and  $u_{ij}$  is the strain, also in Voigt notation. Cuprates have tetragonal ( $D_{4h}$ ) symmetry, and in this work we focus on the uniform compressive strain in the  $xy$  plane, which

is associated to the elastic constant  $c_{A_{1g}} = (c_{11} + c_{22})/2$  of the  $A_{1g}$  irreducible representation. Furthermore, we consider both electronic and lattice degrees of freedom. Hence the free energy is the sum of three terms: the electronic free energy  $F_{\text{el}}$ , the lattice free energy  $F_{\text{latt}}$ , and the free energy due to the interaction between electrons and the lattice  $F_{\text{el-latt}}$ . The elastic constant of the  $A_{1g}$  mode, and hence its associated velocity of sound, is renormalised by the interaction between electrons and lattice as  $c_{A_{1g}}^* = c_{A_{1g}} + \Delta c_{A_{1g}}$ , where  $\Delta c_{A_{1g}}$  is the correction to  $c_{A_{1g}}$  due to electron-lattice interaction, i.e. physically it is the contribution to the elastic stiffness due to the electrons at the Fermi level.

To find  $\Delta c_{A_{1g}}$ , we consider the following Su-Schrieffer-Heeger-Hubbard Hamiltonian<sup>3</sup> on the 2D square lattice:

$$H = - \sum_{ij\sigma} t[a + (d_i - d_j)](c_{i\sigma}^\dagger c_{j\sigma} + c_{j\sigma}^\dagger c_{i\sigma}) + U \sum_i n_{i\uparrow} n_{i\downarrow} - \mu \sum_{i\sigma} n_{i\sigma}. \quad (1)$$

Eq. 1 can be viewed as a *compressible* Hubbard model, as in Refs.<sup>4,5</sup>. Here  $c_{i\sigma}^\dagger, c_{i\sigma}$  create and destroy, respectively, an electron at site  $i$  of spin  $\sigma$ ,  $n_i = c_{i\sigma}^\dagger c_{i\sigma}$  is the number operator,  $U$  is the onsite Coulomb interaction, and  $\mu$  is the chemical potential. Contrary to the (standard) Hubbard model, the nearest neighbor hopping amplitude  $t$  is modulated by the local change  $(d_i - d_j)$  of the equilibrium lattice constant  $a$ , i.e. with zero wavevector as appropriate for ultrasound experiments. This Hamiltonian preserves electroneutrality.

For the 2D compressible Hubbard model with nearest-neighbor hopping in Eq. 1, a lower bound for the correction  $\Delta c_{A_{1g}}$  to the elastic constant  $c_{A_{1g}}$  due to the interaction between electrons and lattice is given by the second derivative of the electronic free energy with respect to hopping,  $\partial^2 F_{\text{el}}/\partial t^2$ , which is proportional to  $\partial(\epsilon)/\partial t$ , where  $t(\epsilon)$  is the kinetic energy of the 2D Hubbard model (see derivation in the supplemental material<sup>25</sup>). This in turn is a lower bound for the velocity of sound of the  $A_{1g}$  mode. To compute this bound, we solve the 2D Hubbard model with the cellular extension<sup>26–28</sup> of dynamical mean-field theory<sup>5</sup>. We solve the cluster -here a  $2 \times 2$  plaquette- with a quantum impurity solver using a continuous time quantum Monte Carlo method<sup>29,30</sup> in the hybridisation expansion of the impurity action. We focus on the normal state only.

*Phase diagram.* – To understand the features of the velocity of sound of the 2D compressible Hubbard model, we briefly review the main aspects of the phase diagram of the underlying 2D Hubbard model. Hole-doped cuprates are doped Mott insulators. To set the system in this regime, we use a value of the interaction larger than threshold  $U_{\text{MIT}}$  necessary to open a Mott gap at zero doping. Figure 1a shows the normal state temperature - doping phase diagram for  $U = 6.2t$  emerging from the CDMFT solution of the 2D Hubbard model<sup>31</sup>. At low temperature there is a first-order transition at finite

doping and finite temperature between a strongly correlated metal with a pseudogap and a correlated metal. This normal state transition is actually hidden beneath a superconducting dome<sup>6,32,34</sup>. It is first-order and ends in a second-order critical endpoint at  $(\delta^*, T^*)$  (gray filled circle). From the endpoint emerge some crossover lines in the thermodynamic<sup>8,9,35</sup> and entanglement<sup>36</sup> properties with the features of the Widom line  $T_W$ . The crossover line defining the onset temperature of the pseudogap  $T^*$  ends abruptly at  $\delta^*$ <sup>9,11</sup>, as found in experiments<sup>37,38</sup>, and is a high-temperature precursor of  $T_W$ . The pseudogap to metal transition is a purely electronic metal to metal transition, and the two phases have the same symmetries.

To reveal the origin of this pseudogap to metal transition without symmetry breaking, it is necessary to vary the interaction  $U$ . Figure 1b shows the  $T - \delta$  phase diagram for  $U = 7.2t$ . Upon increasing  $U$ , the pseudogap to metal transition moves to larger doping and lower temperature. The Widom line can be used to reveal the existence of the pseudogap to metal transition, which in Figure 1b occurs at a low temperature currently inaccessible due to the fermionic sign problem<sup>7</sup>. By further varying the interaction  $U$ , one obtains<sup>6,7</sup> the schematic  $U - \delta$  normal-state phase diagram sketched in Figure 1c. By following the horizontal arrow in the doped Mott insulator regime, the system evolves from a Mott insulator at zero doping to a pseudogap followed by a the first-order transition to a metal. The pseudogap to metal transition (thick gray line) is connected to the metal to Mott insulator transition at zero doping (vertical arrow and the resulting  $U - T$  phase diagram in Figure 1d). This implies<sup>6,7</sup> that the pseudogap to metal transition originates from Mott physics and short-range correlations. Physically, this means Mott localisation plus short range correlations, arising from superexchange, form singlet bonds that open a pseudogap.

The crossing of the Widom line and its underlying second order critical line ending the first-order transition gives rise to a peak in the electronic specific heat<sup>10</sup>. This provides a microscopic framework that solves the apparent paradox raised by recent experiments<sup>2</sup> reporting a sharp peak in the low temperature normal state electronic specific heat at the doping  $\delta^*$  where the pseudogap ends without evidence of broken symmetry states. Our main contribution here is to show that thermodynamic anomalies –such as the peak along the Widom line in the electronic specific heat and in the charge compressibility– are also imprinted in the velocity of sound. We shall show that the isothermal velocity of sound for the  $A_{1g}$  mode has anomalies in the form of sharp dips versus  $\delta$  upon crossing the endpoint of the pseudogap to metal transition and its associated Widom line. Red squares in Figure 1a,b mark the doping levels of the dip in the velocity of sound.

*Velocity of sound in a doped Mott insulator.* – Figure 2a,b shows the lower bound  $\partial^2 F_{\text{el}}/\partial t^2$  for the correction  $\Delta c_{A_{1g}}$  to the elastic constant  $c_{A_{1g}}$  due the electron-lattice interaction, as a function of doping for different

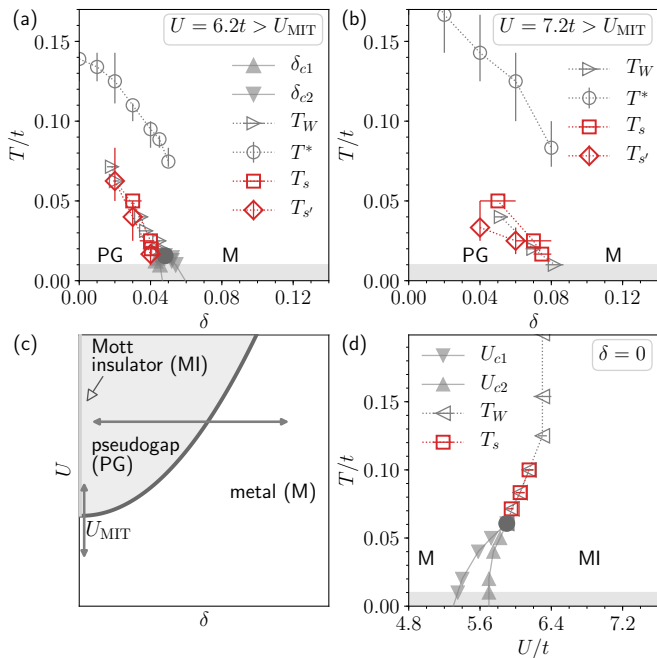


FIG. 1. (a,b) Temperature versus doping normal state phase diagram, as obtained from the CDMFT solution of the 2D Hubbard model (gray symbols). Data are obtained for  $U = 6.2t$  and  $U = 7.2t$ , which set the system in the doped Mott insulator regime. At finite doping there is a first-order phase transition between a pseudogap (PG) and a metal (M). This transition is bounded by the spinodals  $\delta_{c1}$  and  $\delta_{c2}$  (filled triangles) and ends at a critical endpoint (filled dark gray circle). From the endpoint emerges the Widom line,  $T_W$ , here defined as the loci of the peaks in the isothermal charge compressibility  $\kappa$  as a function of doping for different temperatures. The open circles denote where the spin susceptibility drops versus  $T$  at fixed doping, signalling the onset temperature of the pseudogap  $T^*$ . (c) Sketch of the interaction strength  $U$  versus doping normal state phase diagram of the 2D Hubbard model. (d) Temperature versus  $U$  normal state phase diagram for the half filled model ( $\delta = 0$ ). The first-order metal to Mott insulator transition is bounded by spinodals  $U_{c1}$  and  $U_{c2}$  (filled triangles), ending in a critical endpoint (filled circle), from which emanates the Widom line, a supercritical crossover (open triangles) defined by the loci of the inflection in the double occupancy versus  $U$  at fixed  $T$ . Gray symbols are taken from Refs. <sup>31,36</sup>. Red symbols are the new results of this work and indicate the loci of the minima in the velocity of sound versus  $\delta$  at fixed  $T$  (squares in panels a, b) or versus  $U$  at fixed  $T$  (squares in panel d), or versus  $T$  at fixed  $\delta$  (diamonds in panels a, b). These minima are one of the main findings of this article. Shaded area at low  $T$  in panels a, b, d corresponds to the region that is inaccessible because of the fermionic sign problem.

temperatures. This term is proportional to the correction to the velocity of sound for the  $A_{1g}$  mode, and has also been calculated in Ref. <sup>5</sup> in the half-filled case.

The velocity of sound has an anomaly, in the form of a dip with a minimum (indicated by the filled symbols),

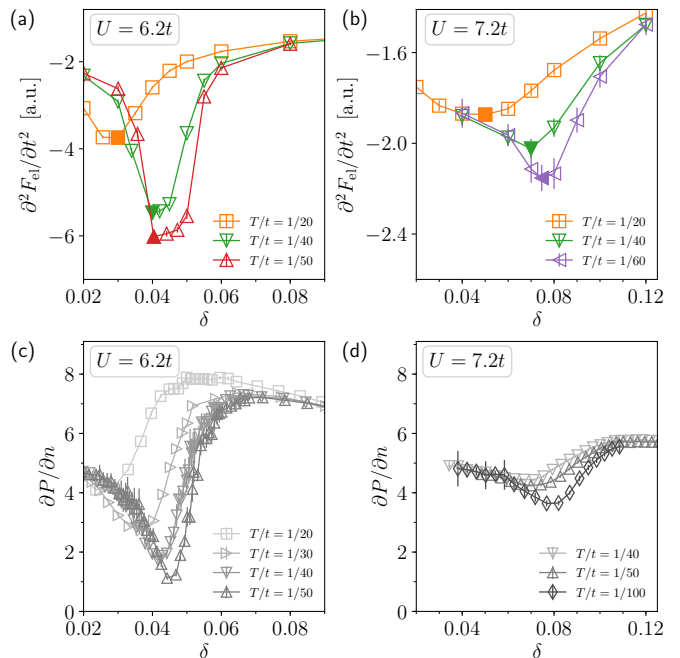


FIG. 2. Upper panels: lower bound for the correction  $\Delta c_{A_{1g}}$  to the elastic constant  $c_{A_{1g}}$  due to the electron-lattice interaction, as a function of doping and for different temperatures. This elastic constant determines the velocity of sound of the  $A_{1g}$  mode. Refer to the supplemental material for the proportionality constants. Minima at finite doping are visible (filled symbols). The loci of the minima vs  $\delta$  of the velocity of sound are shown by red squares ( $T_s$ ) in Fig. 1a,b. Lower panels: velocity of sound of a neutral electron gas  $v_s^2 \propto \partial P / \partial n$ , as a function of doping and for different temperatures. Gray colors emphasise this quantity is at zero strain. Data are shown for  $U = 6.2t$  (panels a, c) and  $U = 7.2t$  (panels b, d). Error bars indicate the rms error.

as a function of doping. The dip becomes more pronounced with decreasing temperature. To understand the origin of this dip, we track the doping levels at which the dips occur for different temperatures. This result is shown in Figure 1a,b on the temperature-doping phase diagram, with red squares. The positions of the dips define a crossover line (open red squares in Figure 1a,b) emerging from the critical endpoint of the pseudogap-metal transition. Therefore, the anomaly in the velocity of sound for the  $A_{1g}$  mode is a signature of the critical point at finite doping and finite temperature and of its associated crossover in the supercritical region.

To further examine the *electronic* origin of the anomalies in the velocity of sound, we calculate the velocity of sound that a neutral electron gas would have  $v_s^2 \propto (\partial P / \partial n)_T$ , where  $P$  is the electronic pressure at zero strain, which is associated with the electronic compressibility  $\kappa = 1/n^2(\partial n / \partial \mu)$  via  $\partial P / \partial n = 1/(n\kappa)$ <sup>31,36</sup>. Figure 2c,d shows the velocity of sound of the electron gas as a function of doping for different temperatures. The curves show a dip that becomes more pronounced as the

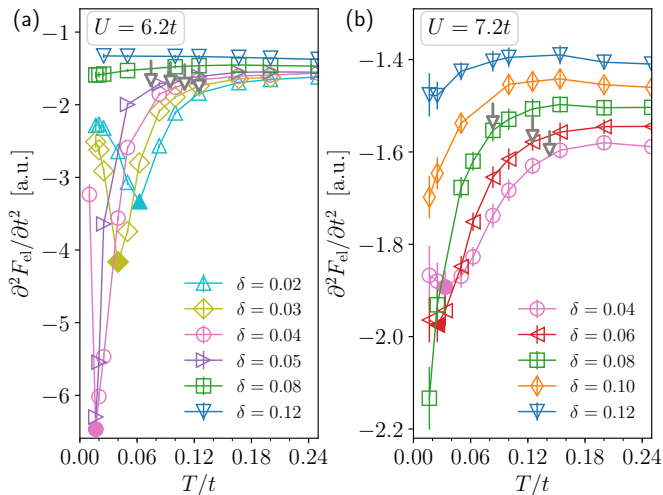


FIG. 3. Lower bound for the correction  $\Delta c_{A_{1g}}$  to the elastic constant  $c_{A_{1g}}$  due to the electron-lattice interaction, as a function of temperature for different values of doping. This quantity is proportional to the velocity of sound of the  $A_{1g}$  mode. Data are obtained for  $U = 6.2t$  (a) and  $U = 7.2t$  (b). The gray arrows indicate the temperature  $T^*$  at each doping level for the underlying 2D Hubbard model (gray open circles in Fig. 1a,b). The curves show a dip (filled symbols) upon crossing the Widom line. The loci of the dips vs  $T$  of the velocity of sound are shown by red diamonds ( $T_{s'}$ ) in Fig. 1a,b. Error bars indicate the rms error.

endpoint is approached. The presence of this minimum in the velocity of sound of the electron gas  $v_s$  suggests an electronic origin of the anomaly in the velocity of sound  $c_s$  for the  $A_{1g}$  mode.

Next, let us discuss the onset temperature of the pseudogap,  $T^*$ , which is a precursory crossover of this metal to metal transition. Because of this, the velocity of sound should be continuous across  $T^*$ . This expectation is fully confirmed by our calculations. Figure 3a,b shows the velocity of sound of the  $A_{1g}$  mode as a function of temperature, for different values of doping. The vertical gray arrows indicate the temperature  $T^*$  at each doping level for the underlying 2D Hubbard model (see Figure 1a,b). Within our numerical uncertainty, the velocity of sound is continuous and does not show any particular features across  $T^*$ . Note that the velocity of sound shows a minimum versus  $T$  (filled symbols in Figure 3a,b and red diamonds in Figure 1a,b) upon crossing the Widom line  $T_W$ .

*Velocity of sound at half filling.*— Since the pseudogap to metal transition is connected to the metal to Mott insulator transition in the interaction-doping plane (Figure 1c), we shall discuss the behavior of the velocity of sound at half filling, across the metal to Mott insulator transition.

The velocity of sound of the  $A_{1g}$  mode has a minimum as a function of  $U/t$  (see Supplemental Material<sup>25</sup>). Most importantly, this minimum defines a crossover line

in the supercritical region (red squares in Figure 1d), which lies close to the Widom line (gray open triangles in Figure 1d). This dip is a signature of the Mott critical point and its associated crossover. This result for the sound velocity versus  $U$  at half filling confirms and extends the findings of Hassan et al.<sup>5</sup> for the 3D compressible Hubbard model solved with single-site DMFT.

*Discussion.*— Using the 2D compressible Hubbard model, we have calculated a lower bound on the isothermal velocity of sound for the  $A_{1g}$  mode with CDMFT, and shown it has a sharp dip versus doping. At low temperature, this anomaly signals a second order critical endpoint at finite temperature and finite doping, which is the endpoint of the pseudogap to metal transition. This is a purely electronic transition without symmetry breaking. Upon increasing  $T$  away from the endpoint, the dip becomes shallower and its locus delineates a supercritical crossover line emanating from the endpoint (red squares in Figure 1a,b).

We predict that ultrasound experiments in hole doped cuprates should observe a minimum in the velocity of sound for the  $A_{1g}$  mode at the doping  $\delta^*$  where the pseudogap ends, once superconductivity is removed by a magnetic field. Furthermore, this dip should become sharper with decreasing temperature. These predicted anomalies indicate the existence of an electronic transition without symmetry breaking, from which supercritical crossovers emerge. This transition is hidden by the superconducting phase<sup>6,32,34,39</sup>. Verifying this prediction in experiments would be a worthy challenge to explore as it may help to unlock the elusive nature of the pseudogap phase.

This dip parallels the peak at  $\delta^*$  in the electronic specific heat recently observed in the LSCO family<sup>2,40</sup> and successfully modeled by the 2D Hubbard model<sup>10</sup>. Given that both specific heat and velocity of sound are thermodynamic indicators of the system, our results provide additional thermodynamic constraints and show that the minimum in the velocity of sound versus  $\delta$  is a likely feature of real materials.

Our prediction for hole doped cuprates is furthermore strengthened by the following observation. The pseudogap to metal transition is connected in the  $U - \delta - T$  space to the metal to Mott insulator transition at zero doping (Figure 1c) where a minimum in the velocity of sound has already been detected in  $V_2O_3$ <sup>19</sup> and in the organic superconductors<sup>5,20</sup>.

While the low temperature crossing of  $\delta^*$  reveals a minimum in the velocity of sound of the  $A_{1g}$  mode versus doping, our calculation shows no signs of a phase transition occurring versus temperature across the onset temperature  $T^*$ . Previous work with ultrasounds<sup>12</sup> reported a break in the slope in the velocity of sound in underdoped YBCO, suggestive instead of a transition at  $T^*$ , but this claim has been challenged in Ref.<sup>13</sup>. We hope that our results may guide further experimental investigations.

## ACKNOWLEDGMENTS

We are indebted to Claude Bourbonnais and Cyril Proust for useful discussions. This work has been supported by the Natural Sciences and Engineering Research

Council of Canada (NSERC) under grants RGPIN-2019-05312, the Canada First Research Excellence Fund and by the Research Chair in the Theory of Quantum Materials. Simulations were performed on computers provided by the Canadian Foundation for Innovation, the Ministère de l'Éducation des Loisirs et du Sport (Québec), Calcul Québec, and Compute Canada.

- 
- \* corresponding author: [giovanni.sordi@rhul.ac.uk](mailto:giovanni.sordi@rhul.ac.uk)
- <sup>1</sup> Cyril Proust and Louis Taillefer, “The remarkable underlying ground states of cuprate superconductors,” *Annual Review of Condensed Matter Physics* **10**, 409–429 (2019).
  - <sup>2</sup> B. Michon, C. Girod, S. Badoux, J. Kačmarčík, Q. Ma, M. Dragomir, H. A. Dabkowska, B. D. Gaulin, J. S. Zhou, S. Pyon, T. Takayama, H. Takagi, S. Verret, N. Doiron-Leyraud, C. Marcenat, L. Taillefer, and T. Klein, “Thermodynamic signatures of quantum criticality in cuprates,” *Nature* **567**, 218–222 (2019).
  - <sup>3</sup> B. Keimer, S. A. Kivelson, M. R. Norman, S. Uchida, and J. Zaanen, “From quantum matter to high-temperature superconductivity in copper oxides,” *Nature* **518**, 179–186 (2015).
  - <sup>4</sup> Henri Alloul, “What is the simplest model that captures the basic experimental facts of the physics of underdoped cuprates?” *Comptes Rendus Physique* **15**, 519 – 524 (2014).
  - <sup>5</sup> Antoine Georges, Gabriel Kotliar, Werner Krauth, and Marcelo J. Rozenberg, “Dynamical mean-field theory of strongly correlated fermion systems and the limit of infinite dimensions,” *Rev. Mod. Phys.* **68**, 13 (1996).
  - <sup>6</sup> G. Sordi, K. Haule, and A.-M. S. Tremblay, “Finite Doping Signatures of the Mott Transition in the Two-Dimensional Hubbard Model,” *Phys. Rev. Lett.* **104**, 226402 (2010).
  - <sup>7</sup> G. Sordi, K. Haule, and A.-M. S. Tremblay, “Mott physics and first-order transition between two metals in the normal-state phase diagram of the two-dimensional Hubbard model,” *Phys. Rev. B* **84**, 075161 (2011).
  - <sup>8</sup> G. Sordi, P. Sémon, K. Haule, and A.-M. S. Tremblay, “Pseudogap temperature as a Widom line in doped Mott insulators,” *Sci. Rep.* **2**, 547 (2012).
  - <sup>9</sup> G. Sordi, P. Sémon, K. Haule, and A.-M. S. Tremblay, “c-axis resistivity, pseudogap, superconductivity, and Widom line in doped Mott insulators,” *Phys. Rev. B* **87**, 041101 (2013).
  - <sup>10</sup> G. Sordi, C. Walsh, P. Sémon, and A.-M. S. Tremblay, “Specific heat maximum as a signature of mott physics in the two-dimensional hubbard model,” *Phys. Rev. B* **100**, 121105 (2019).
  - <sup>11</sup> A. Reymbaut, S. Bergeron, R. Garioud, M. Thénault, M. Charlebois, P. Sémon, and A.-M. S. Tremblay, “Pseudogap, van hove singularity, maximum in entropy, and specific heat for hole-doped mott insulators,” *Phys. Rev. Research* **1**, 023015 (2019).
  - <sup>12</sup> Arkady Shekhter, B. J. Ramshaw, Ruixing Liang, W. N. Hardy, D. A. Bonn, Fedor F. Balakirev, Ross D. McDonald, Jon B. Betts, Scott C. Riggs, and Albert Migliori, “Bounding the pseudogap with a line of phase transitions in  $\text{YBa}_2\text{Cu}_3\text{O}_{6+\delta}$ ,” *Nature* **498**, 75–77 (2013).
  - <sup>13</sup> J. R. Cooper, J. W. Loram, I. Kokanović, J. G. Storey, and J. L. Tallon, “Pseudogap in  $\text{YBa}_2\text{Cu}_3\text{O}_{6+\delta}$  is not bounded by a line of phase transitions: Thermodynamic evidence,” *Phys. Rev. B* **89**, 201104 (2014).
  - <sup>14</sup> Mehdi Frachet, Igor Vinograd, Rui Zhou, Siham Benhabib, Shangfei Wu, Hadrien Mayaffre, Steffen Krämer, Sanath K. Ramakrishna, Arneil P. Reyes, Jérôme Debray, Tohru Kurosawa, Naoki Momono, Migaku Oda, Seiki Komiya, Shimpei Ono, Masafumi Horio, Johan Chang, Cyril Proust, David LeBoeuf, and Marc-Henri Julien, “Hidden magnetism at the pseudogap critical point of a cuprate superconductor,” *Nature Physics* **16**, 1064–1068 (2020).
  - <sup>15</sup> M. Frachet, S. Benhabib, I. Vinograd, S.-F. Wu, B. Vignolle, H. Mayaffre, S. Krämer, T. Kurosawa, N. Momono, M. Oda, J. Chang, C. Proust, M.-H. Julien, and D. LeBoeuf, “High magnetic field ultrasound study of spin freezing in  $\text{La}_{1.88}\text{Sr}_{0.12}\text{CuO}_4$ ,” *Phys. Rev. B* **103**, 115133 (2021).
  - <sup>16</sup> Sayak Ghosh, Michael Matty, Ryan Baumbach, Eric D. Bauer, K. A. Modic, Arkady Shekhter, J. A. Mydosh, Eun-Ah Kim, and B. J. Ramshaw, “One-component order parameter in  $\text{URu}_2\text{Si}_2$  uncovered by resonant ultrasound spectroscopy and machine learning,” *Science Advances* **6**, eaaz4074 (2020).
  - <sup>17</sup> S. Benhabib, C. Lupien, I. Paul, L. Berges, M. Dion, M. Nardone, A. Zitouni, Z. Q. Mao, Y. Maeno, A. Georges, L. Taillefer, and C. Proust, “Ultrasound evidence for a two-component superconducting order parameter in  $\text{Sr}_2\text{RuO}_4$ ,” *Nature Physics* **17**, 194–198 (2020).
  - <sup>18</sup> Sayak Ghosh, Arkady Shekhter, F. Jerzembeck, N. Kikugawa, Dmitry A. Sokolov, Manuel Brando, A. P. Mackenzie, Clifford W. Hicks, and B. J. Ramshaw, “Thermodynamic evidence for a two-component superconducting order parameter in  $\text{Sr}_2\text{RuO}_4$ ,” *Nature Physics* **17**, 199–204 (2020).
  - <sup>19</sup> S. Populoh, P. Wzietek, R. Gohier, and P. Metcalf, “Lattice softening effects at the Mott critical point of Cr-doped  $\text{V}_2\text{O}_3$ ,” *Phys. Rev. B* **84**, 075158 (2011).
  - <sup>20</sup> D. Fournier, M. Poirier, M. Castonguay, and K. D. Truong, “Mott Transition, Compressibility Divergence, and the  $P$ – $T$  Phase Diagram of Layered Organic Superconductors: An Ultrasonic Investigation,” *Phys. Rev. Lett.* **90**, 127002 (2003).
  - <sup>21</sup> Mario Poirier, Maxime Dion, and David Fournier, “Symmetry-imposed signatures at the pseudogap crossover in  $\kappa$ -(BEDT-TTF) $_2X$  organic superconductors,” *Phys. Rev. B* **83**, 132507 (2011).
  - <sup>3</sup> W. P. Su, J. R. Schrieffer, and A. J. Heeger, “Solitons in polyacetylene,” *Phys. Rev. Lett.* **42**, 1698–1701 (1979).
  - <sup>4</sup> Pinaki Majumdar and H. R. Krishnamurthy, “Lattice Contraction Driven Insulator-Metal Transition in the  $d = \infty$  Local Approximation,” *Phys. Rev. Lett.* **73**, 1525–1528 (1994).
  - <sup>5</sup> S. R. Hassan, A. Georges, and H. R. Krishnamurthy, “Sound Velocity Anomaly at the Mott Transition: Application to Organic Conductors and  $\text{V}_2\text{O}_3$ ,” *Phys. Rev. Lett.*

- [94](#), 036402 (2005).
- <sup>25</sup> See Supplemental Material for the derivation of a bound on the velocity of sound  $c_s$  and for additional results of  $c_s$  at half filling.
- <sup>26</sup> Thomas Maier, Mark Jarrell, Thomas Pruschke, and Matthias H. Hettler, “Quantum cluster theories,” *Rev. Mod. Phys.* **77**, 1027–1080 (2005).
- <sup>27</sup> G. Kotliar, S. Y. Savrasov, K. Haule, V. S. Oudovenko, O. Parcollet, and C. A. Marianetti, “Electronic structure calculations with dynamical mean-field theory,” *Rev. Mod. Phys.* **78**, 865 (2006).
- <sup>28</sup> A.-M. S. Tremblay, B. Kyung, and D. Sénéchal, “Pseudogap and high-temperature superconductivity from weak to strong coupling. Towards a quantitative theory,” *Low Temp. Phys.* **32**, 424 (2006).
- <sup>29</sup> Emanuel Gull, Andrew J. Millis, Alexander I. Lichtenstein, Alexey N. Rubtsov, Matthias Troyer, and Philipp Werner, “Continuous-time Monte Carlo methods for quantum impurity models,” *Rev. Mod. Phys.* **83**, 349–404 (2011).
- <sup>30</sup> P. Sémon, Chuck-Hou Yee, Kristjan Haule, and A.-M. S. Tremblay, “Lazy skip-lists: An algorithm for fast hybridization-expansion quantum Monte Carlo,” *Phys. Rev. B* **90**, 075149 (2014).
- <sup>31</sup> C. Walsh, P. Sémon, D. Poulin, G. Sordi, and A.-M. S. Tremblay, “Thermodynamic and information-theoretic description of the Mott transition in the two-dimensional Hubbard model,” *Phys. Rev. B* **99**, 075122 (2019).
- <sup>32</sup> G. Sordi, P. Sémon, K. Haule, and A.-M. S. Tremblay, “Strong Coupling Superconductivity, Pseudogap, and Mott Transition,” *Phys. Rev. Lett.* **108**, 216401 (2012).
- <sup>6</sup> L. Fratino, P. Sémon, G. Sordi, and A.-M. S. Tremblay, “An organizing principle for two-dimensional strongly correlated superconductivity,” *Sci. Rep.* **6**, 22715 (2016).
- <sup>34</sup> Caitlin Walsh, Maxime Charlebois, Patrick Sémon, Giovanni Sordi, and André-Marie S. Tremblay, “Information-theoretic measures of superconductivity in a two-dimensional doped mott insulator,” *Proceedings of the National Academy of Sciences* **118**, e2104114118 (2021).
- <sup>35</sup> C. Walsh, P. Sémon, G. Sordi, and A.-M. S. Tremblay, “Critical opalescence across the doping-driven mott transition in optical lattices of ultracold atoms,” *Phys. Rev. B* **99**, 165151 (2019).
- <sup>36</sup> C. Walsh, P. Sémon, D. Poulin, G. Sordi, and A.-M. S. Tremblay, “Entanglement and classical correlations at the doping-driven mott transition in the two-dimensional Hubbard model,” *PRX Quantum* **1**, 020310 (2020).
- <sup>37</sup> C. Collignon, S. Badoux, S. A. A. Afshar, B. Michon, F. Laliberté, O. Cyr-Choinière, J.-S. Zhou, S. Licciardello, S. Wiedmann, N. Doiron-Leyraud, and Louis Taillefer, “Fermi-surface transformation across the pseudogap critical point of the cuprate superconductor  $\text{La}_{1.6-x}\text{Nd}_{0.4}\text{Sr}_x\text{CuO}_4$ ,” *Phys. Rev. B* **95**, 224517 (2017).
- <sup>38</sup> O. Cyr-Choinière, R. Daou, F. Laliberté, C. Collignon, S. Badoux, D. LeBoeuf, J. Chang, B. J. Ramshaw, D. A. Bonn, W. N. Hardy, R. Liang, J.-Q. Yan, J.-G. Cheng, J.-S. Zhou, J. B. Goodenough, S. Pyon, T. Takayama, H. Takagi, N. Doiron-Leyraud, and Louis Taillefer, “Pseudogap temperature  $T^*$  of cuprate superconductors from the nernst effect,” *Phys. Rev. B* **97**, 064502 (2018).
- <sup>39</sup> L. Fratino, P. Sémon, G. Sordi, and A.-M. S. Tremblay, “Pseudogap and superconductivity in two-dimensional doped charge-transfer insulators,” *Phys. Rev. B* **93**, 245147 (2016).
- <sup>40</sup> C. Girod, D. LeBoeuf, A. Demuer, G. Seyfarth, S. Imajo, K. Kindo, Y. Kohama, M. Lizaire, A. Legros, A. Gourgout, H. Takagi, T. Kurosawa, M. Oda, N. Momono, J. Chang, S. Ono, G.-q. Zheng, C. Marcenat, L. Taillefer, and T. Klein, “Normal state specific heat in the cuprate superconductors  $\text{La}_{2-x}\text{Sr}_x\text{CuO}_4$  and  $\text{Bi}_{2+y}\text{Sr}_{2-x-y}\text{La}_x\text{CuO}_{6+\delta}$  near the critical point of the pseudogap phase,” *Phys. Rev. B* **103**, 214506 (2021).

**Supplemental Material:**  
**Prediction of anomalies in the velocity of sound for the pseudogap of hole-doped cuprates**

C. Walsh, M. Charlebois, P. Sémon, G. Sordi, A.-M. S. Tremblay

In Section I we derive the result for the lower bound on the velocity of sound  $c_s$  of the  $A_{1g}$  mode used in the main text. In Section II we provide additional data for the velocity of sound at half filling.

## I. DERIVATION OF THE LOWER BOUND OF THE VELOCITY OF SOUND

### A. Definitions

The velocity of sound  $c_s$  along high symmetry directions is  $c_s = \sqrt{c_{ij}/\rho}$ , where  $\rho$  is the density and  $c_{ij}$  is the elastic constant in the Voigt notation<sup>1</sup>. Note that  $c_{ij}$  has the units of pressure and is defined as the second derivative of the free energy  $F$  with respect to the strain  $u_{ij}$ ,  $c_{ij} = \partial^2 F / \partial u_{ij}^2$ , with

$$u_{ij} = \frac{1}{2} \left( \frac{\partial u_i}{\partial r_j} + \frac{\partial u_j}{\partial r_i} \right), \quad (1)$$

where  $u_i(\mathbf{r})$  is the displacement along the direction  $r_i$ , with  $(r_1, r_2, r_3) = (x, y, z)$ . Note that the strain  $u_{ij}$  is dimensionless, and thus  $F_{\text{latt}}$  has the units of  $c_{ij}$ , i.e. it is a free energy density.

We want to capture the physics of the cuprates, which have tetragonal crystal structure. Hence we consider the point group  $D_{4h}$ . The resulting lattice free energy  $F_{\text{latt}}$  is<sup>2</sup>

$$F_{\text{latt}} = \frac{1}{2} c_{11} (u_{xx}^2 + u_{yy}^2) + c_{12} u_{xx} u_{yy} + 2c_{66} u_{xy}^2 + \frac{1}{2} c_{33} u_{zz}^2 + c_{13} (u_{xx} + u_{yy}) u_{zz}, \quad (2)$$

with standard Voigt notation for the elastic constants. Furthermore, cuprates are layered materials of 2D planes stacked along the  $z$  axis. We shall calculate the longitudinal velocity of sound within the  $xy$  plane. Hence we consider only the strain in the  $xy$  plane, and neglect the strain in the  $z$  direction. Hence we are left to consider the lattice free energy

$$F_{\text{latt}} = \frac{1}{2} c_{11} (u_{xx}^2 + u_{yy}^2) + c_{12} u_{xx} u_{yy}. \quad (3)$$

Furthermore, we shall consider only uniform compressive strain. Hence, it is useful to write  $F_{\text{latt}}$  using the irreducible representations  $A_{1g}$  and  $B_{1g}$  of  $D_{4h}$  group. The uniform compression is associated with the  $A_{1g}$  mode. The  $A_{1g}$  and  $B_{1g}$  components of the strain can be written as

$$u_{A_{1g}} = u_{xx} + u_{yy} \quad (4)$$

$$u_{B_{1g}} = u_{xx} - u_{yy}. \quad (5)$$

Hence Eq. 3 becomes:

$$F_{\text{latt}} = \frac{1}{2} \left( c_{A_{1g}} u_{A_{1g}}^2 + c_{B_{1g}} u_{B_{1g}}^2 \right), \quad (6)$$

where the elastic constants for the  $A_{1g}$  and  $B_{1g}$  modes are

$$c_{A_{1g}} = \frac{1}{2} (c_{11} + c_{12}) \quad (7)$$

$$c_{B_{1g}} = \frac{1}{2} (c_{11} - c_{12}). \quad (8)$$

Therefore the longitudinal velocity of sound that we shall calculate is

$$c_s = \sqrt{\frac{c_{A_{1g}}}{\rho}}. \quad (9)$$

Up until now we have only considered lattice degrees of freedom. We want to describe both lattice and electronic degrees of freedom, i.e. we want to consider

$$F = F_{\text{latt}} + F_{\text{el}} + F_{\text{el-latt}}. \quad (10)$$

As a result, the velocity of sound  $c_s$  is renormalised by the interaction with the electrons. Hence we can write:

$$c_s = \sqrt{\frac{c_{A_{1g}}^*}{\rho}}, \quad (11)$$

where

$$c_{A_{1g}}^* = c_{A_{1g}} + \Delta c_{A_{1g}}. \quad (12)$$

The correction  $\Delta c_{A_{1g}}$  is coming from the interaction with the electrons. Our goal is thus to find an estimate for  $\Delta c_{A_{1g}}$ .

## B. 2D compressible Hubbard model

To find  $\Delta c_{A_{1g}}$ , we consider the Su-Schrieffer-Heeger (SSH) Hubbard model<sup>3</sup> on a 2D square lattice. To simplify the derivation, we first consider a strain applied in only one direction. Since we consider only nearest neighbor hopping,  $x$  and  $y$  directions are independent. Potential energy is unaffected, so we need only consider how strain modifies the kinetic energy in the direction of the lattice vector where it is applied, hence we have

$$-\sum_{ij\sigma} t[a + (d_i - d_j)](c_{i\sigma}^\dagger c_{j\sigma} + c_{j\sigma}^\dagger c_{i\sigma}), \quad (13)$$

where  $i$  and  $j$  now refer to lattice positions, not cartesian directions as before. We take  $d_i$  as the displacement from equilibrium of the atom at position  $i$ . This model can be also referred to as a *compressible* Hubbard model, as in Refs.<sup>4,5</sup>. Here  $c_{i\sigma}^\dagger$  and  $c_{i\sigma}$  operators create and destroy an electron at site  $i$  of spin  $\sigma$ . The equilibrium distance between atoms is  $a$ . Contrary to the standard Hubbard model, the nearest neighbor hopping amplitude  $t$  in Eq. 13 is not constant, but is modulated by the local change  $(d_i - d_j)$  of the equilibrium lattice constant  $a$ .

A Taylor expansion of the hopping amplitude  $t$  about  $(d_i - d_j) = 0$  gives:

$$t[a + (d_i - d_j)] \approx t_{ij} + \frac{\partial t}{\partial a}(d_i - d_j), \quad (14)$$

where the equilibrium value  $t(a)$  is denoted by  $t_{ij}$ , which is equal to  $t$  for nearest neighbor hopping and to zero otherwise. Therefore the hopping term  $K$  that is modified by  $d_i - d_j$  can be written as:

$$K = K_{\text{el}} + K_{\text{el-latt}} \quad (15)$$

$$= -\sum_{ij\sigma} t_{ij}(c_{i\sigma}^\dagger c_{j\sigma} + c_{j\sigma}^\dagger c_{i\sigma}) - \sum_{ij\sigma} \frac{\partial t}{\partial a}(d_i - d_j)(c_{i\sigma}^\dagger c_{j\sigma} + c_{j\sigma}^\dagger c_{i\sigma}), \quad (16)$$

where  $K_{\text{el}}$  is the familiar hopping term in the standard Hubbard model and  $K_{\text{el-latt}}$  is the modulated hopping term as in a SSH-like model.

It is convenient to take the origin of each bond in the middle of two sites. Along the  $x$  direction then, we rewrite the change in local interatomic distance in terms of the strain, using the notation of the previous subsection in the long wave-length limit

$$d_i - d_{i+1} = -\left. \frac{\partial u_x(\mathbf{r})}{\partial x} \right|_{\mathbf{r}_k} a, \quad (17)$$

where  $\mathbf{r}_k = (\mathbf{r}_{i+1} - \mathbf{r}_i)/2$ , and where index  $k$  labels bonds. We rewrite the second-quantized operators in this basis and define  $\epsilon_x(\mathbf{r}_k)$  as follows

$$c_i^\dagger c_{i+1} = c_{\mathbf{r}_k - a/2}^\dagger c_{\mathbf{r}_k + a/2} = \epsilon_x(\mathbf{r}_k). \quad (18)$$

because stretched bonds are in the  $x$  direction.

Then the electron-lattice interaction  $K_{\text{el-latt}}$  in Eq. 16 along the  $x$  direction becomes

$$\sum_{x_k} \left( -a \frac{\partial t}{\partial a} \right) u_{xx}(\mathbf{r}_k) \left( c_{\mathbf{r}_k - a/2}^\dagger c_{\mathbf{r}_k + a/2} + h.c. \right) = g \sum_{x_k} u_{xx}(\mathbf{r}_k) (\epsilon_x(\mathbf{r}_k) + h.c.), \quad (19)$$

with the definition

$$g = -a \frac{\partial t}{\partial a}. \quad (20)$$

The result is similar in the  $y$  direction. Note that  $g > 0$  because  $t$  decreases when  $a$  increases, and that  $g$  has units of energy.

Next we move to reciprocal space assuming a single wave-vector. And since we consider uniform compressive strain we will eventually take the  $q \rightarrow 0$  limit. Taking the Fourier transform of the strain gives:

$$u_{xx}(\mathbf{r}_k) = u_{xx}(\mathbf{q}) (e^{i\mathbf{q}\cdot\mathbf{r}} + e^{-i\mathbf{q}\cdot\mathbf{r}}) / 2, \quad (21)$$

where  $\mathbf{q}$  is in the  $x$  direction and  $q \rightarrow 0$ . Then the interaction Eq. 19 becomes (since  $u_{xx}(q) = u_{xx}(-q)$ ):

$$g \frac{u_{xx}(q)}{2} (\epsilon_x^-(q) + \epsilon_x^+(q)) + g \frac{u_{xx}(-q)}{2} (\epsilon_x^-(q) + \epsilon_x^+(q)), \quad (22)$$

with a similar result in the  $y$  direction. Here  $\epsilon^+$  and  $\epsilon^-$  denote the two terms entering the kinetic energy. Both  $u_{xx}(q)$  and  $\epsilon_x^\pm$  are dimensionless.

Bringing together the terms along the  $x$  and  $y$  directions, we obtain:

$$K_{\text{el-latt}} = g [\epsilon_x(-q)u_{xx}(q)/2 + \epsilon_x(q)u_{xx}(-q)/2] + g [\epsilon_y(-q)u_{yy}(q)/2 + \epsilon_y(q)u_{yy}(-q)/2], \quad (23)$$

where we defined:

$$\epsilon_x(q) = \epsilon_x^-(q) + \epsilon_x^+(q) \quad (24)$$

$$\epsilon_y(q) = \epsilon_y^-(q) + \epsilon_y^+(q). \quad (25)$$

Our aim is to trace over the electronic degrees of freedom to find out how  $F_{\text{latt}}$  is modified. For completeness then, let us also write  $F_{\text{latt}}$  in reciprocal space. For clarity, let us focus only on  $u_{xx}$  with a single wave-vector as above. We find

$$F_{\text{latt}} = \int \frac{1}{2} c_{11} u_{xx}(\mathbf{r}) u_{xx}(\mathbf{r}) d\mathbf{r} = \frac{1}{2} c_{11} \frac{u_{xx}(q) u_{xx}(-q)}{2}. \quad (26)$$

### C. A bound to the correction to the elastic free energy from coupling to the conduction electrons

We take the following steps, valid only for a Hubbard model with nearest neighbor hopping. First we find the correction to the elastic free-energy to second-order in  $g$  for a simple strain  $u_{xx}$ . We obtain a zero-frequency Matsubara response function as the correction, a result identical to what we would have obtained from a phonon self-energy-calculation for this model. Second, we bound this result with an equal-time correlation function. Third we trivially extend the result to a  $A_{1g}$  strain. Finally, we rewrite the result for the correction to the elastic constant  $c_{A_{1g}}$  in terms of a derivative of the kinetic energy.

#### 1. Perturbative result for the free energy

The contribution to the elastic stiffness due to the conduction electrons is obtained by tracing over them. In other words, in this section we are focusing on the contributions to the partition function that comes from the electronic Hamiltonian and from the interaction of the electrons with the lattice. We assume that the elastic free energy without the conduction electrons is already known.

As before, we can separate the strains along the  $x$  and  $y$  direction. Let us focus on the  $x$  direction. We take the strain  $u_{xx}$  as a *classical* variable that commutes with the electronic Hamiltonian. Therefore, in the interaction representation, the partition function  $Z$  is:

$$Z = \text{Tr}_{\text{el}} \left[ e^{-\beta H_{\text{el}}} T_\tau e^{-\int_0^\beta d\tau g [\epsilon_x(-q, \tau) u_{xx}(q)/2 + \epsilon_x(q, \tau) u_{xx}(-q)/2]} \right], \quad (27)$$

where  $T_\tau$  is the imaginary-time ordering operator,  $H_{\text{el}}$  is the electronic Hamiltonian that includes the Hubbard term, and the operator  $\epsilon_x(q, \tau)$  in imaginary time is given by the usual Heisenberg time evolution

$$\epsilon_x(-q, \tau) = e^{H_{\text{el}}\tau} \epsilon_x(-q) e^{-H_{\text{el}}\tau}. \quad (28)$$

Expanding the exponential to second order, we obtain:

$$Z = Z_{\text{el}} \left\langle 1 - \int_0^\beta d\tau g [\epsilon_x(-q, \tau) u_{xx}(q)/2 + \epsilon_x(q, \tau) u_{xx}(-q)/2] + \frac{1}{2} \int_0^\beta d\tau \int_0^\beta d\tau' g^2 [\epsilon_x(-q, \tau) \epsilon_x(q, \tau') u_{xx}(q) u_{xx}(-q)/2] \right\rangle. \quad (29)$$

Here the brackets refer to a thermal average with the electronic Hamiltonian. We also used that  $\langle \epsilon_x(-q) \epsilon_x(-q) \rangle = 0$ , so that only  $\langle \epsilon_x(q) \epsilon_x(-q) \rangle$  survives. We can also now take the  $q \rightarrow 0$  limit without worrying because  $\epsilon_x$  is not conserved, so the  $q \rightarrow 0$  limit and the zero-frequency limit can be taken in any order. Finally, the contribution to the free energy from the conduction electrons is given by

$$F = -\frac{1}{\beta} \ln Z = F_{\text{el}} - \frac{1}{\beta} \ln [\langle 1 \rangle - g \langle X \rangle + g^2 \langle Y \rangle], \quad (30)$$

where

$$X = \int_0^\beta d\tau \epsilon_x(\tau) u_{xx} \quad (31)$$

is first order in  $u_{xx}$  and

$$Y = \int_0^\beta d\tau \int_0^\beta d\tau' \epsilon_x(\tau) \epsilon_x(\tau') u_{xx} u_{xx} / 2 \quad (32)$$

is second order in  $u_{xx}$ . Expanding the natural logarithm to second order in  $g u_{xx}$  we thus obtain:

$$F = F_{\text{el}} - \frac{1}{\beta} \left[ g \langle -X \rangle + g^2 \langle Y \rangle - \frac{g^2}{2} \langle X \rangle^2 \right]. \quad (33)$$

The first term in the square brackets is a shift of the zero of the strain. Substituting the above definitions of  $X$  and  $Y$  in the last equation, we are left with

$$F = F_{\text{el}} - \frac{g^2}{\beta} \left[ \int_0^\beta d\tau \int_0^\beta d\tau' \langle \epsilon_x(\tau) \epsilon_x(\tau') \rangle - \left[ \int_0^\beta d\tau \langle \epsilon_x(\tau) \rangle \right]^2 \right] \frac{u_{xx} u_{xx}}{2}. \quad (34)$$

The cyclic property of the trace, equivalently time-translation invariance, leads to  $\langle \epsilon_x(\tau) \rangle = \langle \epsilon_x \rangle$  independent of  $\tau$ . The same reasoning allows us to rewrite the first term as well, so that the previous equation takes the form

$$F = F_{\text{el}} - g^2 \left[ \int_0^\beta d\tau \langle \epsilon_x(\tau) \epsilon_x(0) \rangle - \beta \langle \epsilon_x \rangle^2 \right] \frac{u_{xx} u_{xx}}{2}. \quad (35)$$

The renormalization of the elastic constant that one can read from this equation is exactly what one would have obtained from the polarization operator for the self-energy of phonons in the nearest neighbor SSH-Hubbard model for  $q \rightarrow 0$ . In general this is the quantity we should compute. It is quite complicated to do this calculation rigorously including vertex corrections. We are going to find a bound that is more convenient to obtain numerically and that contains vertex corrections.

## 2. Establishing a bound

The quantity in brackets of the last equation is the zero bosonic Matsubara frequency component of the more general correlation function

$$\chi_{\epsilon_x, \epsilon_x}(i\omega_n) = \int \frac{d\omega}{\pi} \frac{\chi''_{\epsilon_x, \epsilon_x}(\omega)}{\omega - i\omega_n}, \quad (36)$$

where the Fourier transform of  $\chi''_{\epsilon_x, \epsilon_x}(\omega)$  in real time  $t$  is given by the commutator

$$\chi''_{\epsilon_x, \epsilon_x}(t) = \frac{1}{2} \langle [\epsilon_x(t), \epsilon_x] \rangle. \quad (37)$$

Using the elementary equality  $[\epsilon_x(t), \epsilon_x] = -[\epsilon_x, \epsilon_x(t)]$  for a commutator and then time-translational invariance  $\langle[\epsilon_x, \epsilon_x(t)]\rangle = \langle[\epsilon_x(-t), \epsilon_x]\rangle$ , we conclude that  $\chi''_{\epsilon_x, \epsilon_x}(\omega)$  is an odd function of frequency ( $\chi''_{\epsilon_x, \epsilon_x}(t)$  is real for a real Hamiltonian). The expression for  $\chi_{\epsilon_x, \epsilon_x}(i\omega_n)$  then becomes

$$\chi_{\epsilon_x, \epsilon_x}(i\omega_n) = \int \frac{d\omega}{\pi} \frac{\omega \chi''_{\epsilon_x, \epsilon_x}(\omega)}{\omega^2 + \omega_n^2}. \quad (38)$$

On the other hand, the equal-time correlation function is given by

$$\langle \epsilon_x(0) \epsilon_x(0) \rangle - \langle \epsilon_x \rangle^2 = \frac{1}{\beta} \sum_n \chi_{\epsilon_x, \epsilon_x}(i\omega_n). \quad (39)$$

Since all terms in the expression for the susceptibility in Matsubara frequency  $\chi_{\epsilon_x, \epsilon_x}(i\omega_n)$  in Eq. 38 are positive, the zero Matsubara frequency contribution is an upper bound

$$\langle \epsilon_x^2 \rangle - \langle \epsilon_x \rangle^2 < \frac{1}{\beta} \chi_{\epsilon_x, \epsilon_x}(i\omega_n = 0). \quad (40)$$

Using this result, the bound on the order  $g^2$  result for the correction to the free-energy Eq. 35 becomes

$$F > F_{\text{el}} - \beta g^2 [\langle \epsilon_x^2 \rangle - \langle \epsilon_x \rangle^2] \frac{u_{xx}^2}{2}. \quad (41)$$

### 3. Response to the $A_{1g}$ mode

By applying a uniform strain in both the  $x$  and  $y$  directions, we can find the response to a  $A_{1g}$  mode. First, we invert Eqs. 4, 5 and find

$$u_{xx} = (u_{A_{1g}} + u_{B_{1g}})/2 \quad (42)$$

$$u_{yy} = (u_{A_{1g}} - u_{B_{1g}})/2. \quad (43)$$

Rewriting the coupling of the strain in both directions in terms of irreducible representations, we find

$$u_{xx}\epsilon_x + u_{yy}\epsilon_y = \frac{1}{2}u_{A_{1g}}(\epsilon_x + \epsilon_y) + \frac{1}{2}u_{B_{1g}}(\epsilon_x - \epsilon_y). \quad (44)$$

If we have only  $u_{A_{1g}}$ , we couple to the total kinetic energy at  $q \rightarrow 0$ . We can redo the above derivation to compute the correction to the free energy for a  $A_{1g}$  mode. The steps are identical. Hence we find

$$F > F_{\text{el}} - \frac{g^2}{4}\beta [\langle \epsilon^2 \rangle - \langle \epsilon \rangle^2] \frac{1}{2}u_{A_{1g}}^2, \quad (45)$$

which is valid only for nearest neighbors, as we have already mentioned, i.e. for

$$\epsilon = \epsilon_x(q=0) + \epsilon_y(q=0) \quad (46)$$

$$= 2 \sum_{k\sigma} (\cos k_x a + \cos k_y a) c_{k\sigma}^\dagger c_{k\sigma}. \quad (47)$$

### 4. Evaluating the bound from a derivative of the kinetic energy

Finally, we can evaluate the bound from a derivative of the expectation value for the kinetic energy. The expectation value of  $\epsilon$  is

$$\langle \epsilon \rangle = \frac{\text{Tr} [\epsilon e^{-\beta[-t\epsilon+V]}]}{\text{Tr} [e^{-\beta[-t\epsilon+V]}]}, \quad (48)$$

where  $V$  contains the Hubbard interaction and the chemical potential contribution. This can be computed from the partition function using a partial derivative

$$\langle \epsilon \rangle = \frac{1}{\beta} \frac{\partial}{\partial t} \ln Z. \quad (49)$$

Taking one more derivative, we find

$$\frac{1}{\beta^2} \frac{\partial^2}{\partial t^2} \ln Z = \frac{1}{\beta} \frac{\partial}{\partial t} \langle \epsilon \rangle = \langle \epsilon^2 \rangle - \langle \epsilon \rangle^2. \quad (50)$$

Substituting this last result in our bound for the free energy Eq. 45, we find

$$F > F_{\text{el}} - \frac{g^2}{4} \frac{\partial \langle \epsilon \rangle}{\partial t} \frac{1}{2} u_{A_{1g}}^2. \quad (51)$$

Therefore, the correction  $\Delta c_{A_{1g}}$  to the elastic constant  $c_{A_{1g}}$  due to the electron-lattice interaction is

$$\Delta c_{A_{1g}} = \frac{\partial^2 F}{\partial u_{A_{1g}}^2} \quad (52)$$

$$> -\frac{g^2}{4} \frac{\partial \langle \epsilon \rangle}{\partial t} \Big|_{U, T, \mu}, \quad (53)$$

which, using  $F_{\text{el}} = -\log Z/\beta$  and Eq. 50 may be rewritten as

$$\Delta c_{A_{1g}} > \frac{g^2}{4} \frac{\partial^2 F_{\text{el}}}{\partial t^2}. \quad (54)$$

This has units of energy density as required. In Eq. 53 we have specified explicitly that the partial derivative is at constant  $U, T, \mu$ .

We compute the derivative  $\partial \langle \epsilon \rangle / \partial t$  in Eq. 53 using centered differences with respect to  $t$ , with a mesh of  $\Delta t = 0.005$ . To obtain the kinetic energy  $t \langle \epsilon \rangle$  we use the method described in Ref. 6.

## II. EXTENDED DATA FOR THE VELOCITY OF SOUND AT HALF FILLING

In this section we present additional data supporting that the estimate for the velocity of sound of the  $A_{1g}$  mode shows a minimum versus  $U/t$  at half filling. Figure S1 shows the velocity of sound of the  $A_{1g}$  mode as a function of  $U/t$  at half filling ( $\delta = 0$ ) and for different temperatures. The curves show a minimum versus  $U/t$  (filled symbols). The position of the minima are shown as red squares in Figure 1 of the main text.

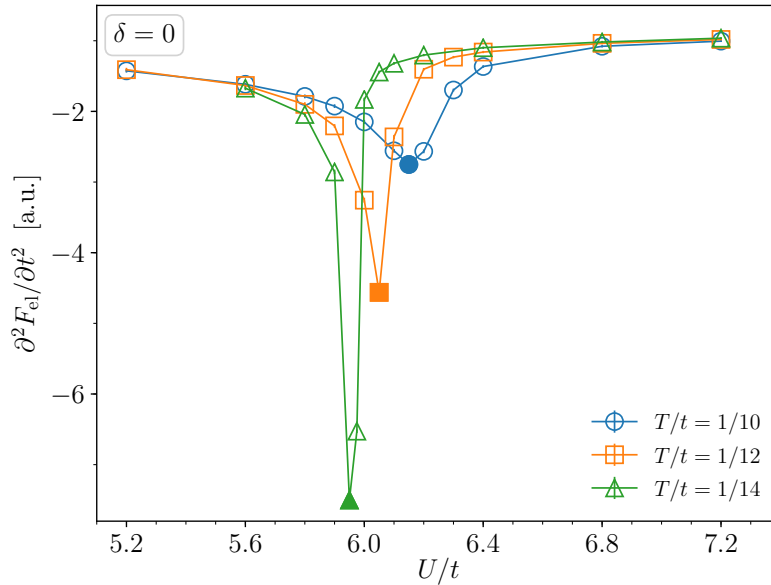


FIG. S1. Lower bound for the correction  $\Delta c_{A_{1g}}$  to the elastic constant  $c_{A_{1g}}$  due to the electron-lattice interaction, at half filling ( $\delta = 0$ ) as a function of  $U/t$  and for different temperatures. A minimum at finite  $U$  and finite  $T$  is visible (filled symbols). The loci of the minima of the velocity of sound are shown by red squares in the  $T - U$  phase diagram of Fig. 1d of the main text.

---

\* corresponding author: [giovanni.sordi@rhul.ac.uk](mailto:giovanni.sordi@rhul.ac.uk)

- <sup>1</sup> L. D. Landau, L. P. Pitaevskii, E. M. Lifshitz, and A. M. Kosevich, *Theory of Elasticity*, 3rd ed. (Butterworth-Heinemann, Oxford, 1986).
- <sup>2</sup> S. Benhabib, C. Lupien, I. Paul, L. Berges, M. Dion, M. Nardone, A. Zitouni, Z. Q. Mao, Y. Maeno, A. Georges, L. Taillefer, and C. Proust, *Nature Physics* , 1–5 (2020).
- <sup>3</sup> W. P. Su, J. R. Schrieffer, and A. J. Heeger, *Phys. Rev. Lett.* **42**, 1698 (1979).
- <sup>4</sup> P. Majumdar and H. R. Krishnamurthy, *Phys. Rev. Lett.* **73**, 1525 (1994).
- <sup>5</sup> S. R. Hassan, A. Georges, and H. R. Krishnamurthy, *Phys. Rev. Lett.* **94**, 036402 (2005).
- <sup>6</sup> L. Fratino, P. Sémon, G. Sordi, and A.-M. S. Tremblay, *Sci. Rep.* **6**, 22715 (2016).